REFERENCE

IC/65/44

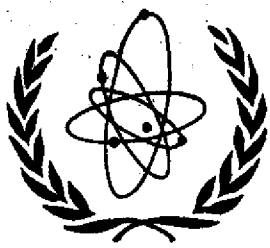

FOR THEORETICAL PHYSICS
MAY 1965
LIBRARY

INTERNATIONAL ATOMIC ENERGY AGENCY

INTERNATIONAL CENTRE FOR THEORETICAL PHYSICS

ISOBAR DIAGRAMS AND INELASTIC RESONANCE PRODUCTION

G. F. WOLTERS

1965

PIAZZA OBERDAN

TRIESTE

IC/65/44

INTERNATIONAL ATOMIC ENERGY AGENCY

INTERNATIONAL CENTRE FOR THEORETICAL PHYSICS

ISOBAR DIAGRAMS AND INELASTIC RESONANCE PRODUCTION*

G. F. WOLTERS **

TRIESTE

May 1965

* To be submitted to Nuovo Cimento

** On leave of absence from the Zeeman Laboratory, University of Amsterdam, Amsterdam, Netherlands.

SUMMARY

Experimental results for the reactions $K^-p \rightarrow Y_1^{*\pm}(1385)\pi^{\pm}$ and a few other reactions in the few GeV energy region are discussed. Qualitative arguments are given in favour of an interpretation of certain non-peripheral features in terms of isobar diagrams. Subsequently the reaction $K^-p \rightarrow pK^{*-}(888)$ is analysed in a more rigorous approach based on the assumption that, at large momentum transfers at least, K^* production through an intermediate isobar is dominant. This analysis is based on well-established conservation laws, without making use of dynamical assumptions. As a result it is shown that the data at 1.5 GeV/$_c$ incident momentum are consistent with the one isobar hypothesis applied in the backward hemisphere of the overall cm-system, for isobar spin $\frac{5}{2}$ and positive parity. The amplitudes for disintegration of the intermediate isobar into the final state are approximately determined, up to some ambiguities in phase.

1. INTRODUCTION

In the few GeV energy region the salient features observed in $K^{\pm}p$ and $\pi^{\pm}p$ reactions, yielding final states containing one or more resonances, are as has been noted by many authors: a marked tendency for formation of quasi two body final states; preference for small momentum transfers; significant structure in the resonance disintegration angular distribution. The third feature is compatible with disintegration of the resonance as a free particle.

Similar features have been observed in NN reactions and in pion photoproduction from nucleons. Although the peripheral model[1] in suitable adaptations, meets with considerable success in accounting for these features[2], attention is drawn to the fact that in the phenomenological analysis of photoproduction of pions from nucleons in the energy region of the higher nucleon isobars, besides one meson exchange diagrams isobar diagrams turned out to be necessary[3]. Then one might a fortiori expect that such diagrams can play a distinct role in $K^{\pm}N$ and $\pi^{\pm}N$ reactions too, since here the coupling between the incident meson and the intermediate isobars is in general stronger than in photoproduction reactions.

In this article mainly $K\bar{p}$ reactions will be considered in view of examining whether known experimental data contain evidence for isobar diagram contributions.

As concerns the peripheral model, it has been noticed in particular that the third feature, mentioned above, allows one to specify to some extent the appropriate model: the spin density matrix of the resonance can be determined partially, and from this knowledge e. g. the ratio of pseudoscalar meson exchange to vector meson exchange amplitudes follows[4]. The application of resulting models for predicting the resonance production angular distributions yielded some discrepancy with the observed distributions, in particular at and above 3 GeV, the last ones showing stronger forward peaking. This difficulty has been removed by taking into account absorptive effects, due to competing

channels[5]. Since this modification of the peripheral model does not change the predicted resonance spin density matrix in a crucial way, satisfactory agreement both with the observed resonance production angular distribution and its disintegration characteristics could be obtained. A different formulation of this modification in terms of the K-matrix, imposing the unitarity condition on the S-matrix, which reduces the Born terms in low partial waves, is due to DIETZ and PILKUHN[6].

Meanwhile, it is realized that even these refined peripheral models do not account for the observed features at all momentum transfers in certain reactions, nor are they applicable to all reactions possible, e. g. in $\bar{K}p$ collisions. Also if three or more particle final states (non-resonant background), are somehow taken into account explicitly, such as in Dietz and Pilkuhn's model, where a statistical treatment is applied to such states, this difficulty remains. It is the purpose of this article to draw attention to a few such non-peripheral features in $\bar{K}p$ reactions, and to consider the possibility of relating these features to isobar diagrams. In Section 2 this will be done in a rather qualitative way, whereas in Section 3 a more detailed study follows of the reaction $\bar{K}p \rightarrow pK^{*-}(888)$. Also here the K^* production angular distribution and its disintegration angular distribution will be predicted, and comparison with experimental data will be made.

2. SOME EMPIRICAL REMARKS ON $\bar{K}p$ REACTIONS

The major part of this section is devoted to the reactions $\bar{K}p \rightarrow Y_1^{*\pm}\pi^{\mp}$ at 1.5 GeV/$_c$ incident momentum (Lab). At the end of the section some other reactions will briefly be considered.

Not all phenomena observed in the Y_1^* production reactions have been interpreted in a satisfactory way[7]. In part, large statistical uncertainties in the measured production angular distribution, Y_1^* disintegration angular distribution, Λ polarisation etc. obscure the true structure. Nevertheless some typical nonperipheral features

are well established experimentally. These features will be discussed below.

The notation $\hat{A}$ to indicate the unit vector along the 3 momentum of particle A in the overall rest system, is adopted. Sometimes $\hat{A}$ will be taken in another reference frame, which will then be stated explicitly.

The experiment[6] shows some backward peaking of Y_1^*, which is roughly equal for the two charge states. Since one meson exchange cannot contribute to Y_1^{*-} production, this is no argument in favour of important peripheral production of Y_1^{*+}. Actually a much more pronounced forward peaking of the Y_1^*'s is observed. This effect is most important for Y_1^{*-}; for both charge states inclusion of negative fourth order terms in $(\hat{K}^-\hat{Y}_1^*)$ is necessary for the fit to the production angular distribution. No peripheral model, with reasonable choices of form factors, reproduces this structure[1]. From the density distribution in the Dalitz plot one estimates that 5 per cent of the events in the resonance mass bands correspond to non-resonant final states[8]. The background amplitude appears to be too small to account for the observed deviation of the production angular distribution from predicted forms in a peripheral model.

A second indication for the presence of a non-peripheral production mechanism comes from what might be called the $\rho\frac{1}{2}(Y_1^*)$ anomaly. The Y_1^* spin alignment along the direction of motion of the incident K-meson, $\hat{K}^-$ seen in a Y_1^* rest system, which direction is taken as a z-axis in that rest system, is specified by $\rho\frac{1}{2}(Y_1^*)$, measuring the population of $J_z = \pm\frac{1}{2}$ Y_1^* spin states. It is assumed that $Y_1^*(1385)$ has spin $\frac{3}{2}$. The experiment reveals that $\rho\frac{1}{2}(Y_1^*)$ is significantly smaller than one for Y_1^* production angles, such that $|(\hat{K}^-Y_1^*)| \geq 0.85$. More precisely one has $\rho\frac{1}{2}(Y_1^{*+}) \simeq 0.4 \pm 0.1$, respectively $\rho\frac{1}{2}(Y_1^{*-}) \simeq 0.65 \pm 0.10$ for $|(\hat{K}^-\hat{Y}_1^*)| \geq 0.85$. The same orders of magnitude are found when less collimated Y_1^*'s are also considered. (Statistics prevented consideration of more collinated Y_1^*'s : for $|(\hat{K}^-\hat{Y}_1^*)| \geq 0.96$ one is left with 14 Y_1^{*+}'s and with 20 Y_1^{*-}'s.) The anomaly consists of a discrepancy with the expectation $\rho\frac{1}{2}(Y_1^{*+}) \simeq 1$ for $|(\hat{K}^-\hat{Y}_1^*)| \geq 0.85$ if peripheral production were dominant. The exchanged

K^* would leave invariant the z-component of the baryon spin. Again the effect appears to be too large to be due to interference with the background amplitude. If the non-resonant $\Lambda\pi^+$ system would have angular momentum with exclusively $J_z \neq \pm\frac{1}{2}$, which would be the most favourable case for such an explanation, the background amplitude, necessary besides one meson exchange amplitude still amounts to 40 per cent or more. The argument is further supported by the fact that the observed Y_1^* disintegration angular distribution in the polar angle of $\hat{\Lambda}$, taken in the Y_1^* rest system, does not show any deviation from symmetry. Finally the argument is not invaliditated by some indications[7] in the observed Y_1^* disintegration angular distribution in the azimuthal angle and in the distribution of the Λ polarization, as a function of the polar angle of $\hat{\Lambda}$, for disturbing interference effects, since these distributions refer to quantities that entirely depend on interference between different amplitudes and are much more sensitive to disturbing interference effects.

The measured values of $\rho_{\frac{1}{2}}(Y_1^*)$ necessarily require orbital angular momenta $\ell \geq 2$ of the $Y_1^*\pi$ system to be important, once final state interactions are neglected[9]. The well-known argument that at production angles θ and $\pi-\theta$ quasi two-body final states with $\ell\theta < 1$ have $J_z = \pm\frac{1}{2}$ for the baryon, yields this lower bound. The result is consistent with the occurrence of fourth order terms in the Y_1^* production angular distribution.

On account of the properties of the Y_1^* production angular distribution and the alignment of the Y_1^* spin, discussed above, one infers that a non-peripheral production mechanism is indeed active, rather than assuming dominant peripheral production, and putting the blame for the $\rho_{\frac{1}{2}}(Y_1^*)$ anomaly on the account of final state interactions[7]. In fact a natural interpretation follows immediately if isobar diagrams are introduced. Just as in the phenomenological analysis of photo production reactions[8], one may think of uncrossed and crossed Born diagrams, indicated in Figs. 1.a and 1.b respectively These diagrams represent the simplest possible non-peripheral mechanism.

The uncrossed Born diagram, in which the intermediate isobar may have isospin 0 or 1, leads to identical contributions to the $Y_1^{*\pm}$ production angular distributions, which moreover are symmetric in $(\hat{K}^-\hat{Y}_1^*)$. The observed distributions contain considerable symmetric parts. Introducing the function $R(\cos\theta) = \frac{W(\cos\theta) - W(-\cos\theta)}{W(\cos\theta) + W(-\cos\theta)}$, where $\cos\theta = (\hat{K}^-\hat{Y}_1^*)$ and W stands for the best fit to the observed distribution[7], one has for the two charge states of Y_1^* that have been considered in the experiment:

$\cos\theta$	0.25	0.50	0.75	1
$R(Y_1^{*+})$	0.45	0.50	0.37	0.12
$R(Y_1^{*-})$	0.19	0.31	0.38	0.45

These values illustrate that in $W(Y_1^{*+})$ as well as in $W(Y_1^{*-})$ the symmetric parts are more important than the antisymmetric parts, the last ones not being negligible on the other hand. If this is taken as a plausibility argument to assume that the uncrossed diagram effectively contributes, at the same time a diagram of different type is needed to account for the asymmetry in $W(Y_1^{*\pm})$. The fact that everywhere on $0 \leq \cos\theta \leq 1$ $R(Y_1^{*\pm})$ is positive implies that such a diagram favours forward Y_1^* production. This immediately leads to the crossed diagram as a plausible candidate. It is then interesting to notice, that in the $Y_1^{*-}\pi^+$ channel the intermediate isobar N^* can have isospin $\frac{1}{2}$ or $\frac{3}{2}$, but that in the $Y_1^{*+}\pi^-$ channel only isospin $\frac{3}{2}$ is allowed in the crossed diagram. One may conjecture that the different behaviour of $R(Y_1^*)$ for the two charge states, and in particular the more pronounced forward peaking of Y_1^{*-}, are directly related to this difference in possible crossed diagrams. Of course also interference between several diagrams can be different for the two Y_1^* charge states.

As concerns the uncrossed diagram, it has to be required that the spin of the intermediate isobar, called $J(Y^*)$, satisfies the condition $J(Y^*) \geq \frac{5}{2}$ in order to allow for the fourth order terms in $W(Y_1^*)$. For $J(Y^*) = \frac{5}{2}$ and even respectively odd parity of the intermediate isobar one then disposes of p-and f-wave Y_1^* production amplitudes,

respectively d- and g-wave amplitudes, for the uncrossed diagram. This combined with presence of crossed diagrams, which leads to $Y_1^*\pi$ states without a limitation on allowed ℓ-values, seems to be sufficient to account for the observed low values of $\rho_{\frac{1}{2}}(Y_1^{*\pm})$, discussed before. A comparable example, where a sole uncrossed diagram with p- and f-wave amplitudes yields an amount of spin alignment which is less than half the value predicted on the basis of one pseudoscalar meson exchange, for production angles near 0 or π, will be treated in Section 3.

It need hardly be emphasized that the tentative interpretation of the salient features observed for the process considered above, based on an isobar-peripheral model rather than a peripheral model, is preliminary. Neither the available data, nor the arguments used in their interpretation, lead to conclusive results at present. The type of analysis to be performed in a somewhat more quantitative approach, is well known. An example is a recent study of some associated production reactions at comparable energies, in which both isobar diagrams and one meson exchange diagrams are taken into account explicitly[10]. Here a few general remarks on the appropriate isobar-peripheral model are made only.

In order to obtain a manageable model one is tempted to restrict oneself to the nearest singularities of the production amplitude. The total CM energy being $\simeq 2$ GeV, this leads to identifying tentatively the intermediate isobar in Fig.1.a with Y_0^* (1815). This isobar probably possesses spin and parity $J^P = \frac{5}{2}^+$ [11]. Also Y_1^* (1765) might contribute, with $J^P = \frac{5}{2}^-$. Study of the reaction $\bar{K}N \to Y_1^*\pi$ will enable one to determine the relative weights of the two diagrams. In Fig.1.b one is led to identify N^* with N respectively $N_{\frac{3}{2}}^*$ (1238) as plausible candidates. Adjustable parameters in the isobar model are effective coupling constant products and partial widths. Results for these parameters will be important for comparison with predictions from symmetry schemes.

Contributions due to K^* exchange cannot a priori be excluded; at a higher energy such contributions are known to be dominant. Cf. remarks below. Finally, as mentioned before, certain observable

quantities may be sensitive to the influence of non-resonant final states.

The model will lead to predictions of the Y_1^* production differential cross-section and the joint final state density matrix, as functions of energy.

Secondly, the type of useful experimental information will thus be: production cross-sections, production angular distributions, Y_1^* disintegration angular distributions in polar and azimuthal angle and Λ polarization over the range of incident momenta 1.3 - 1.7 GeV/$_c$ at least. Similar data for the reaction $\bar{K}n \to Y_1^* \pi$ will be of importance. As concerns the Y_1^* disintegration characteristics, separation of the Y_1^* sample according to some intervals of production angle corresponding to increasing four-momentum transfer is desirable, in order to gain better insight into the role of peripheral contributions presumably present mainly at the smallest momentum transfers, and of contributions from crossed isobar diagrams, presumably present mainly at the largest momentum transfers occurring in the reaction.

A less ambitious approach consists of selecting reactions for which the number of possible contributing diagrams is smaller than for $\bar{K}p \to Y_1^* \pi$. Evidence for isobar diagrams may then be contained already in a smaller amount of experimental data, e.g. data for fixed total energy, and their contributions may be studied conveniently.

As a first example $\bar{K}p$ reactions at 3 GeV/$_c$ incident momentum (Lab) may be mentioned. Besides final states which are definitely produced peripherally, such as $n\bar{K}^0$; $\Sigma^+\pi^-$; $\Lambda\pi^0$; $\Lambda\eta$; $Y_1^{*+}\pi^-$ and pK^{*-}, also final states are observed, with smaller cross-sections, in which the baryon moves preferably in forward directions. Examples are $\Sigma^-\pi^+$; $Y_1^{*-}\pi^+$; Ξ^-K^+ and Ξ^-K^{*+} [12]. Uncrossed isobar diagrams seem to be negligible at this momentum, whereas one meson exchange is excluded. It appears therefore that these reactions are entirely due to crossed isobar diagrams, if the simplest possible mechanism is again preferred instead of more complicated ones that might be invented. From this point of view these reactions are obviously important and worth studying in great detail both experimentally and theoretically.

An a priori more complicated example is provided by reactions of the type $K^+p \to NK^*$; N^*K or N^*K^*. Here uncrossed isobar diagrams are forbidden, if no strangeness +1 isobar exists at least. Data at 1.5 GeV/$_c$ incident momentum (Lab) have been analysed in a peripheral model with form factors[13]. To the author's knowledge no attempt has been made to consider crossed isobar diagrams explicitly, in addition to one meson exchange diagrams. Data at 3GeV/$_c$ seem to be consistent with dominant peripheral production, with absorptive effects taken into account[14]. In view of these results and the results for $\bar{K}p$ reactions at this same high momentum, it thus turns out that at 3 GeV/$_c$ isobar diagrams probably are not competitive with peripheral diagrams in $K^\pm p$ reactions. Their precise influence is unknown.

A third example is the reaction $\bar{K}p \to pK^{*-}$, where crossed isobar diagrams are forbidden. According to the previous remark and the discussion of the reactions $\bar{K}p \to Y_1^* \pi$, one may expect that K^{*-} production as indicated, at 1.5 GeV/$_c$, provides evidence for the presence of intermediate isobars Y_0^* (1815) or Y_1^*(1675), besides possibly one meson exchange. This process is therefore suitable for examining more critically than has been done so far, if further evidence for the "isobar-peripheral" model can be obtained, in spite of the limited experimental data available. The following section deals with this problem.

3 STUDY OF THE REACTION $\bar{K}p \to pK^{*-}$ AT 1.5 GeV/$_c$ INCIDENT MOMENTUM

The experimental results of an investigation of the reaction $\bar{K}p \to pK^{*-}(888)$ at 1.5 GeV/$_c$ incident momentum (Lab)[15,16], as far as they are relevant for the following analysis, are recalled here:

(a) The histogram for the K^{*-} production angular distribution in the overall CM system, shown in Fig. 2. Forward K^{*-} production is dominant, but in addition a peak in the backward hemisphere is present. Its maximum lies between $(\hat{\bar{K}}.\hat{K}^{*-}) = -0.6$ and $= -0.8$.

It is possible[16] to consider this distribution $W(K^{*-})$ as a sum of a purely peripheral distribution, which is taken identical to the known distribution $W(K^{*+})$ for the reaction $K^+p \to pK^{*+}$ at 1.5 GeV/c, and a remaining symmetric distribution. If statistics will be improved, this decomposition may turn out to be an over-simplification. In any event, one can assert that experiment suggests that peripheral diagrams are present, together with an uncrossed isobar diagram, the respective contributions of which to $W(K^{*-})$ may add incoherently approximately. The peak near $(\hat{K}^-.\hat{K}^{*-}) = \pm 0.7$ in the isobar contribution requires this contribution to be at least of the 4th order in $(\hat{K}^-.\hat{K}^{*-})$, so the intermediate isobar has spin $\frac{5}{2}$ or more. Moreover the isobar diagram dominates in the backward hemisphere.

(b) The K^{*-} spin density matrix ρ, as far as determined by the K^* disintegration angular distribution. Three intervals of four momentum transfer squared have been considered separately, which intervals correspond to a partition of the whole $(\hat{K}^-.\hat{K}^{*-})$ interval into three equal subintervals. Use is made of a K^* rest system, in which the z-axis lies along $\hat{K}^-$, seen in the K^* rest system, while the y-axis is perpendicular to the production plane. The system is right-handed. The following parameters are defined:

$$\lambda = -2\,\mathrm{Re}\,\rho_{1,0} \;;\; \mu = \mathrm{Im}\left(\rho_{1,0} - \rho_{0,-1}\right) \;;\; \nu = \mathrm{Re}\,\rho_{1,-1} \;;\; \sigma = -\mathrm{Im}\,\rho_{1,-1} \quad (1)$$

Invariance with respect to reflection through the production plane requires μ and σ to be zero. The experimental results, integrated over each one of the three subintervals, are consistent with $\mu = \sigma = 0$. Moreover the K^* disintegration angular distribution actually can be fitted satisfactorily with an expression characteristic for spin 1 of K^*. Hence no indication of disturbing interference is present. The results for the remaining free parameters, $\rho_{0,0}$, λ and ν are as follows:

TABLE I.

	$\frac{1}{3} \leq (\hat{\bar{K}}.\hat{K}^{*-}) \leq 1$	$-\frac{1}{3} \leq (\hat{\bar{K}}.\hat{K}^{*-}) \leq \frac{1}{3}$	$-1 \leq (\hat{\bar{K}}.\hat{K}^{*-}) \leq -\frac{1}{3}$
$\rho_{0,0}$	0.56 ± 0.08	0.16 ± 0.11	0.27 ± 0.10
λ	-0.09 ± 0.10	-0.04 ± 0.13	0.29 ± 0.12
ν	-0.02 ± 0.07	0.05 ± 0.10	-0.20 ± 0.09

As has been noted,[15] the apparent difference between the values in the last column and those in the preceding columns again suggests that different production mechanisms are present in the backward respectively forward hemisphere. The simplest possible interpretation is that on the interval $-1 \leq (\hat{\bar{K}}.\hat{K}^{*-}) \leq -\frac{1}{3}$ peripheral contributions can be neglected altogether. The corresponding data thus are accessible to an extremely simple approach, in which one uncrossed isobar diagram is assumed to be present only.

It is pointed out now, that according to this hypothesis the consequences of K^{*-} production, through an intermediate state of definite spin and parity can be analysed, on the basis of well-established conservation laws, without performing a dynamical analysis in the framework of dispersion theory of perturbation theory. It can thus be verified in a solid way if the hypothesis is consistent with the mentioned data. However no prediction of energy dependence can then be made. As soon as similar data at not too remote K^-momenta become available dynamical calculations will be necessary to obtain further evidence concerning the "one isobar hypothesis". Obviously also in the forward hemisphere the dynamical approach cannot be avoided.

The first part of the analysis in the backward hemisphere consists of the derivation of the expressions for $W(K^{*-})$ and the matrix ρ in terms of the amplitudes for the disintegration $Y^* \rightarrow pK^{*-}$. This derivation may be reviewed here in the helicity representation.

As a starting point the general expression for the final state joint spin density matrix is written down[17]:

$$\rho_{\lambda_{K^*},\lambda_p;\lambda'_{K^*},\lambda'_p} = \frac{2J+1}{4\pi} T_{\lambda_{K^*},\lambda_p} T^*_{\lambda'_{K^*},\lambda'_p} \times$$

$$\sum_{M,M'} \rho_{M,M'}(Y^*)\, e^{i(M-M')\varphi}\, d^J_{M,\lambda}(\theta)\, d^J_{M',\lambda'}(\theta) \quad (2)$$

Here J is the Y^* spin, with z-component M; $\rho(Y^*)$ is the Y^* spin density matrix; $T_{\lambda_{K^*},\lambda_p}$ are helicity amplitudes. Making use of axial symmetry around $\bar{K}$, which direction defines the z-axis in the Y^* rest system (the orientation of the x- and y-axis need not be specified for this system), a more convenient expression reads:

$$\rho_{\lambda_{K^*},\lambda_p;\lambda'_{K^*},\lambda'_p} = T_{\lambda_{K^*},\lambda_p} T^*_{\lambda'_{K^*},\lambda'_p} \times$$

$$\sum_{M=\frac{1}{2}}^{J} \{ \rho_M(Y^*)\, Q^+(J,M,\lambda,\lambda',\theta) + \delta_M(Y^*)\, Q^-(J,M,\lambda,\lambda',\theta) \} \quad (3)$$

In Eq. (3) the $\rho_M(Y^*)$ are the Y^* spin alignment parameters, whereas

$$\delta_M(Y^*) = \rho_{M,M}(Y^*) - \rho_{-M,-M}(Y^*)$$

The functions $Q^\pm$, depending on the polar angle of $\hat{K}^*$, called θ as before, are defined as follows:

$$Q^\pm(J,M,\lambda,\lambda',\theta) = \sum_{\ell=0}^{2J} \tfrac{1}{2}(1\pm(-1)^\ell) R(J,M,\lambda,\lambda',\ell)\, P_\ell^{\lambda-\lambda'}(\theta) \quad (4)$$

where P_ℓ^{m}s are associated Legendre polynomials. The coefficients R expressed in terms of 3j symbols[18], are given by:

$$R(J,M,\lambda,\lambda',\ell) = (-1)^{M-\lambda'}(J+\tfrac{1}{2})(2\ell+1)\sqrt{\frac{(\ell-\lambda+\lambda')!}{(\ell+\lambda-\lambda')!}} \times$$

$$\begin{pmatrix} J & J & \ell \\ M & -M & 0 \end{pmatrix} \begin{pmatrix} J & J & \ell \\ \lambda & -\lambda' & -\lambda+\lambda' \end{pmatrix} \quad (5)$$

They are a generalization of angular distribution coefficients extensively studied elsewhere[19]. The functions $Q^{\pm}$ have simple symmetry properties:

$$Q^{\pm}(J, M, \lambda', \lambda, \theta) = \pm Q^{\pm}(J, -M, \lambda, \lambda', \theta) =$$
$$\pm (-1)^{\lambda-\lambda'} Q^{\pm}(J, M, -\lambda, -\lambda', \theta) = \pm (-1)^{\lambda-\lambda'} Q^{\pm}(J, M, \lambda, \lambda', \pi-\theta)$$
$$= Q^{\pm}(J, M, \lambda, \lambda', \theta) \qquad (6)$$

For obtaining Eq. (3) use has been made of Eq. (6). Since the intermediate isobar has "Adair spin alignment", $\rho_M = \delta_{M\frac{1}{2}}$, and the initial protons can be assumed to be unpolarised, $\delta_M(Y^*) = 0$, Eq. (3) simplifies to

$$\rho_{\lambda_{K^*}, \lambda_p; \lambda'_{K^*}, \lambda_p} = T_{\lambda_{K^*}, \lambda_p} T^*_{\lambda'_{K^*}, \lambda'_p} Q^{+}(J, \tfrac{1}{2}, \lambda, \lambda', \theta) \qquad (7)$$

This result holds irrespective as to whether parity is conserved or not. On account of Eq. (6) the joint spin density matrix is hermitian. Moreover since parity is conserved, which implies that the helicity amplitudes are not all independent:

$$T_{-\lambda_{K^*}, -\lambda_p} = \eta\, T_{\lambda_{K^*}, \lambda_p}$$
$$\eta = P(Y^*)(-1)^{J-\frac{1}{2}} \qquad (8)$$

it follows from Eqs. (6), (7) and (8):

$$\rho_{-\lambda_{K^*}, -\lambda_p; -\lambda'_{K^*}, -\lambda'_p} = (-1)^{\lambda'-\lambda} \rho_{\lambda_{K^*}, \lambda_p; \lambda'_{K^*}, \lambda'_p} \qquad (9)$$

Finally the K^* production angular distribution W and the K^* spin density matrix $\rho^{K^*}(\theta)$ are obtained from Eq. (7) by taking the full trace respectively the trace with respect to the proton helicity variable, of the joint spin density matrix. Adopting the notation:

$$Q^+(\gamma, \tfrac{1}{2}, \lambda, \lambda', \theta) = Q_{2\lambda, 2\lambda'} \tag{10}$$

one finds making use of Eq. (8):

$$W = 2\left\{\left|T_{1,\frac{1}{2}}\right|^2 + \left|T_{0,\frac{1}{2}}\right|^2\right\} Q_{1,1} + 2\left|T_{1,-\frac{1}{2}}\right|^2 Q_{3,3} \tag{11}$$

respectively

$$\begin{aligned}
\rho^{K^*}_{1,1}(\theta) &= \left|T_{1,\frac{1}{2}}\right|^2 Q_{1,1} + \left|T_{1,-\frac{1}{2}}\right|^2 Q_{3,3} \\
\rho^{K^*}_{0,0}(\theta) &= 2\left|T_{0,\frac{1}{2}}\right|^2 Q_{1,1} \\
\rho^{K^*}_{1,0}(\theta) &= \eta\, T_{1,-\frac{1}{2}}\, T^*_{0,\frac{1}{2}}\, Q_{3,1} + T_{1,\frac{1}{2}}\, T^*_{0,\frac{1}{2}}\, Q_{1,-1} \\
\rho^{K^*}_{1,-1}(\theta) &= 2\eta\, \mathrm{Re}\left\{T_{1,\frac{1}{2}}\, T^*_{1,-\frac{1}{2}}\right\} Q_{3,-1}
\end{aligned} \tag{12}$$

Since ρ^{K^*} satisfies a relation similar to Eq. (9), which is usually formulated as invariance under reflection through the production plane, and as ρ^{K^*} is hermitian it is sufficient to give the four elements in Eq. (12) in order to specify the whole matrix ρ^{K^*}. It may be noted that $Q_{1,-1}$ identically vanishes on account of Eq. (6).

Before comparison with the mentioned data can be made, some elementary transformations have to be applied to ρ^{K^*} as it stands in Eq. (12). First of all ρ^{K^*} and the experimentally determined matrix ρ refer to different reference systems. These two K^* rest systems

are related by the rotation about the common y-axis, which turns $\hat{K}^*$ into $\hat{K}^-$, both vectors taken in the K^* rest frame. The angle of rotation Θ is a function of θ. Subsequently the matrix obtained after applying this rotation has to be integrated over the chosen interval of production angles. Finally the resulting matrix has to be divided by the total probability to find a K^* at one of the production angles thus selected, which leads to $\mathrm{Tr}\,\rho = 1$.† Taking the result, Eq. (C. 2) and introducing for convenience the combination of parameters $1-\rho_{0,0} \pm 2\nu$ and $-\sqrt{2}\lambda$, recalling Eq. (1), one deals with the expressions:

$$
\begin{aligned}
1-\rho_{0,0}+2\nu &= D^{-1}2\Big[\,|T_{1,\frac{1}{2}}|^2 S_{1,1} + |T_{1,-\frac{1}{2}}|^2 S_{3,3} + \\
&\qquad + 2\eta\, \mathrm{Re}\{T_{1,\frac{1}{2}} T^*_{1,-\frac{1}{2}}\} S_{3,-1}\Big] \\
1-\rho_{0,0}-2\nu &= D^{-1}2\Big[\,|T_{1,\frac{1}{2}}|^2 S^{(2)}_{1,1} + |T_{1,-\frac{1}{2}}|^2 S^{(2)}_{33} + \\
&+ 2|T_{0,\frac{1}{2}}|^2\{S_{1,1}-S^{(2)}_{1,1}\} - 2\eta\, \mathrm{Re}\{T_{1,\frac{1}{2}} T^*_{1,-\frac{1}{2}}\} S^{(2)}_{3,-1} + \\
&\qquad + \sqrt{2}\,\eta\, \mathrm{Re}\{T_{1,-\frac{1}{2}} T^*_{0,\frac{1}{2}}\} S^{(1)}_{3,1}\Big] \\
-\sqrt{2}\,\lambda &= D^{-1}\Big[-|T_{1,\frac{1}{2}}|^2 S^{(1)}_{1,1} - |T_{1,-\frac{1}{2}}|^2 S^{(1)}_{3,3} + \\
&+ 2\eta\, \mathrm{Re}\{T_{1,\frac{1}{2}} T^*_{1,-\frac{1}{2}}\} S^{(1)}_{3,-1} - 2\sqrt{2}\,\eta\, \mathrm{Re}\{T_{1,-\frac{1}{2}} T^*_{0,\frac{1}{2}}\} \times \\
&\{S_{3,1} - 2S^{(2)}_{3,1}\} + 2|T_{0,\frac{1}{2}}|^2 S^{(1)}_{1,1}\Big]
\end{aligned}
\tag{13}
$$

The denominator D is given by Eq. (C. 1). The integrals S, defined in appendix B, are further discussed in appendix D. Eq. (13) is general, i. e. it can be applied to find the pure isobar contributions to $\rho_{0,0}$, λ and ν as functions of the three independent helicity amplitudes, on any interval of production angles. Moreover the results (11) and (13) hold for an arbitrary value of the isobar spin J.

Next comes the comparison of Eqs. (11) and (13) with the mentioned data.

† These transformations are discussed in Appendices A, B and C.

To start with, the K^* production angular distribution, normalized according to $\int_{-1}^{1} d\cos\theta\, W = 1$, is considered. From Eqs. (4) and (5) it follows that

$$\int_{-1}^{1} d\cos\theta\; Q_{2\lambda,2\lambda} = 2R(\gamma, M, \lambda, \lambda, 0) = 1$$

So the choice of normalization is equivalent to:

$$\sum_{\lambda_{K^*},\lambda_p} \left| T_{\lambda_{K^*},\lambda_p} \right|^2 = 1$$

on account of Eq. (11). Introducing the new parameter

$$T = 2\left|T_{1,\frac{1}{2}}\right|^2 + 2\left|T_{0,\frac{1}{2}}\right|^2 \qquad (14)$$

one concludes that the isobar hypothesis implies a severe restriction on W : this distribution depends on one adjustable real parameter T only, instead of the three helicity amplitudes. Of course one disposes, in addition, of a scale factor N, which will be chosen so that $\int_{-1}^{\rho} d\cos\theta W$ is equal for the theoretical and observed distributions. The restriction on possible shapes of W depends on the value of J. Of primary interest is the case $J = \frac{5}{2}$. In this case computation of $Q_{1,1}$ and $Q_{3,3}$ leads to the result:

$$W = N\{1 + a\cos^2\theta + b\cos^4\theta\} \quad \text{with}$$

$$a = -2\,\frac{9T-7}{T+1} \quad \text{and} \quad b = 5\,\frac{5T-3}{T+1} \qquad (15)$$

Hence the coefficients a and b are not independent:

$$4b = 5(2-a) \qquad (16)$$

The observed presence of a maximum in W near $\cos\theta = -\sqrt{\frac{1}{2}}$ completely fixes T on account of Eqs. (15) and (16), except for the statistical uncertainty in the position of the maximum. A priori it has to be required that the resulting T value should lie between 0 and 1, which obviously is the case. Unfortunately T varies rapidly with the position of the maximum. Fig. 2 shows the curves for W plotted on $-1 \leq \cos\theta \leq 1$, for different choices of T. The curves 1, 2, 3, 4 correspond to T = 0.37, 0.28, 0.14 and 0 respectively. A conservative conclusion is that the isobar hypothesis is compatible with the observed distribution when

$$0 \leqslant T \lesssim 0.37 \tag{17}$$

Subsequently the data quoted in Table I are considered. In view of Eq. (13) the measured parameters $\rho_{0,0}$, λ and ν depend on four real almost independent parameters, which may be chosen as follows:

$$\begin{aligned} t &= 2\left|T_{0,\frac{1}{2}}\right|^2 \\ s &= \sqrt{2}\,\eta\, Re\left\{T_{1,-\frac{1}{2}}\, T^*_{0,\frac{1}{2}}\right\} \\ r &= 2\eta\, Re\left\{T_{1,\frac{1}{2}}\, T^*_{1,-\frac{1}{2}}\right\} \end{aligned} \tag{18}$$

the remaining parameter being T defined by Eq. (14). This time the isobar hypothesis imposes restrictions on possible values of $\rho_{0,0}$, λ and ν by virtue of the general constraints

$$\begin{aligned} &0 \leqslant t \leqslant T \leqslant 1 \\ &|s| \leqslant \sqrt{\tfrac{1}{2} t\,(1-T)} \\ &|r| \leqslant \sqrt{(T-t)(1-T)} \end{aligned} \tag{19}$$

In principle knowledge of $W, \rho_{0,0}, \lambda, \nu$ is sufficient to determine r, s, t and T and comparison of the solution with Eqs. (17) and (19) provides a consistency criterion for the isobar hypothesis. Again the considerable statistical uncertainty in the experimental data may allow for some set of solutions, satisfying Eqs. (17) and (19). This actually turns out to be the case. Before discussing in more detail the results of the fits to the data, one other general remark may be made, which concerns the determination of the helicity amplitudes from solutions for r, s, t and T. As is evident from Eqs. (14) and (18) these amplitudes are determined by a given solution up to an irrelevant common phase, complex conjugation and the ambiguity defined by invariance under the simultaneous substitutions

$$T_{1,\frac{1}{2}} \to -T_{1,\frac{1}{2}} \; ; \; T_{0,\frac{1}{2}} \to -T_{0,\frac{1}{2}} \; ; \; T_{1,-\frac{1}{2}} \to T_{1,-\frac{1}{2}} \text{ and } \eta \to -\eta \quad \text{†)}.$$

Hence the parity of the intermediate isobar cannot be determined from the quoted measured parameters for ρ and from W. Either the transverse proton polarization in the final state has to be measured for this purpose, or some dynamical assumption has to be made in addition. It can be shown that only the second possibility applies. At the end of this section a crude centrifugal barrier argument will be considered.

The results of the data analysis on the interval $-1 \leq \cos\theta \leq -\frac{1}{3}$ will be discussed next. Inserting the corresponding numerical values of the integrals S for $J = \frac{5}{2}$ into Eq. (13) and taking the constraints (17) and (19) into account, the isobar model predicts as possible ranges for the values of $\rho_{0,0}, \lambda$ and ν :

$$\begin{aligned} 0.05 &\leq \rho_{0,0} \leq 0.50 \\ -0.20 &\leq \nu \leq 0.33 \\ -0.14 &\leq \lambda \leq 0.46 \end{aligned} \qquad (20)$$

† A general discussion of ambiguities in elastic scattering amplitudes has recently been given by R. Van WAGENINGEN, Annals of Physics 31, (1965) 148. However in this paper only "unpolarized" cross-sections have been considered. The ambiguity found here may be generalized along the same lines as followed by Van Wageningen.

Allowing for one standard deviations (certainly) the values in the last column of Table I are consistent with Eq. (20). Violation of Eq. (20) would have ruled out the isobar hypothesis; the actual result encourages further investigation of the acceptable solutions. Eq. (13) defines the functions $\rho_{0,0}(r,s,t,T)$; $\nu(r,s,t,T)$ and $\lambda(r,s,t,T)$, and one is led to consider the customary quantity

$$X^2 = \left(\frac{\rho_{0,0} - 0.27}{0.10}\right)^2 + \left(\frac{\nu + 0.20}{0.09}\right)^2 + \left(\frac{\lambda - 0.29}{0.12}\right)^2$$

constructed from these functions and the measured values. For T fixed X^2 has been minimized taking the constraints (17) and (19) into account. The resulting best solutions r(T), s(T) and t(T) together with their X^2 values are displayed in Fig. 3. This picture shows that solutions for $T \lesssim 0.10$ may be rejected. Then the orders of magnitude of r and s are reasonably well defined for the optimal fits, but variations of the order of 0.05 in r and s are compatible with $X^2 \lesssim 2$ on the remaining interval $0.10 \lesssim T \lesssim 0.37$. It is interesting to notice that the curve r(T) in Fig. 3 represents the maximal values of r allowed. So a characteristic property of the optimal solutions is that $T_{1,\frac{1}{2}}$ and $T_{1,-\frac{1}{2}}$ have the same phase. In view of the undeterminancy in r corresponding to $X^2 \lesssim 2$, it cannot be proved that the two K^* helicity 1 amplitudes interfere exhaustively, but at least strong interference is predicted.

As mentioned in connection with W, it does not seem possible to interpret data in the forward hemisphere in terms of one uncrossed isobar diagram. Therefore application of the analysis just outlined to the data present in the second column of Table I, is expected to yield either inconsistency with Eq. (19) or solutions which are significantly different from the ones obtained on $-1 \leq \cos\theta \leq -\frac{1}{3}$. As a matter of fact the second alternative prevails. The best solution in an absolute sense, for $0 \leq T \leq 0.37$, reads: $r = -0.07$, $s = -0.28$, $t = 0.25$ and $T = 0.37$. Its X^2 is 0.9, which may be compared with the absolute minimum $X^2 = 0.05$ for $-1 \leq \cos\theta \leq -\frac{1}{3}$. A search for best simultaneous solutions for $-1 \leq \cos\theta \leq -\frac{1}{3}$ and $-\frac{1}{3} \leq \cos\theta \leq \frac{1}{3}$ leads to $X > 13$ for such fits, everywhere for $0 \leq T \leq 0.37$.

It is concluded that, within the limits of the present non-dynamical approach, the data at the largest momentum transfers can be satisfactorily interpreted in terms of K^* production through a spin $\frac{5}{2}$ intermediate isobar. Energetically $Y_o^*(1815)$ is the most plausible candidate for the isobar. At smaller momentum transfers no such interpretation is possible, which is attributed to competing peripheral diagrams. From the fits to the present data, on the interval $-1 \leq \cos\theta \leq -\frac{1}{3}$, the helicity amplitudes, describing the disintegration $Y^* \rightarrow pK^*$, might be determined approximately and up to some ambiguities in phases. Higher precision in the data is needed for an accurate determination of the helicity amplitudes, which in turn will provide valuable information concerning the Y^*NK^* coupling. Moreover knowledge of these amplitudes will facilitate the analysis of the data at smaller momentum transfers, in the framework of an "isobar-peripheral" model. Here some common features of the acceptable solutions for the helicity amplitudes may be mentioned, without going into details. Fig. 3 contains almost all the necessary information for obtaining details.

For $X^2 \lesssim 2$ $T_{1,-\frac{1}{2}}$ is the largest amplitude and $T_{0,\frac{1}{2}}$ and $T_{1,\frac{1}{2}}$ are of the same order of magnitude. The relative phase of $T_{1,-\frac{1}{2}}$ and $T_{1,\frac{1}{2}}$ is zero or finite and small for $P(Y^*) = +$, which is sufficient to characterize also the solutions for opposite parity. The relative phase of $T_{0,\frac{1}{2}}$ and $T_{1,-\frac{1}{2}}$ is of the order of $60^\circ \pm 30^\circ$

The corresponding ℓS amplitudes; p_3, f_3 and f_1 for $P(Y^*) = +$, and d_3, g_3, d_1 for opposite parity, are readily obtained[17]. Being mainly interested in their magnitudes, it is sufficient to mention that $|p_3| > |f_3| > |f_1|$ respectively $|d_3| > |g_3| \approx |d_1|$. Some solutions exist for which $|f_3| \approx |f_1|$ respectively $|g_3| < |d_1|$. At each inequality maximal differences in magnitude are of the order of a factor 2.5.

Evidently none of the solutions for $P(Y^*) = \pm$ is in clear contradiction with what might be expected on the basis of the centrifugal barrier effect. However it is pointed out that in particular for the optimal solutions one has $|g_3| \approx |d_1|$, whereas always $|p_3| > |f_3|$. This is a weak indication in favour of $P(Y^*) = +$, supporting the hypothesis $Y^* = Y_o^*(1815)$.

Appendix A

The K^* rest system to which $\rho^{K^*}(\theta)$, Eq. (12), refers has its z-axis along $\hat{K}^*$ and its y-axis perpendicular to the production plane. It is right-handed. In order to obtain the matrix ρ partially determined in the experiment, this reference system is rotated about the y-axis over an angle Θ such that the new z-axis points along $\hat{K}^-$, seen in the K^* rest system. The K^* production angle θ, $\cos\theta = \hat{K}^- . \hat{K}^*$, is defined in the overall cm system. Hence $\Theta \neq \theta$ but Θ is a known function of θ to be specified in Appendix D. In this appendix the transformed matrix

$$\rho^{K^*}(\Theta, \theta) = d^1(-\Theta)\, \rho^{K^*}(\theta)\, d^1(\Theta) \tag{A.1}$$

will be given. Using the same convention as Jacob and Wick for the definition of the d-functions[17], one has

$$\rho^{K^*}_{1,\pm1}(\Theta, \theta) = \rho^{K^*}_{1,1}(\theta) + \rho^{K^*}_{1,-1}(\theta) \pm \rho^{K^*}_{0,0}(\theta) \pm \sqrt{2}\, \mathrm{Re}\, \rho^{K^*}_{1,0}(\theta) \sin 2\Theta$$
$$\pm \left\{ \rho^{K^*}_{1,1}(\theta) - \rho^{K^*}_{1,-1}(\theta) - \rho^{K^*}_{0,0}(\theta) \right\} \cos^2\Theta$$

$$\rho^{K^*}_{0,0}(\Theta, \theta) = 2\left\{ \rho^{K^*}_{1,1}(\theta) - \rho^{K^*}_{1,-1}(\theta) \right\} - 2\sqrt{2}\, \mathrm{Re}\, \rho^{K^*}_{1,0}(\theta) \sin 2\Theta$$
$$- \left\{ \rho^{K^*}_{1,1}(\theta) - \rho^{K^*}_{1,-1}(\theta) - 2\rho^{K^*}_{0,0}(\theta) \right\} \cos^2\Theta$$

$$\rho^{K^*}_{1,0}(\Theta, \theta) = -2\left\{ \rho^{K^*}_{1,0}(\theta) \right\}^* + \tag{A.2}$$
$$- \tfrac{1}{2}\sqrt{2} \left\{ \rho^{K^*}_{1,1}(\theta) - \rho^{K^*}_{1,-1}(\theta) - \rho^{K^*}_{0,0}(\theta) \right\} \sin 2\Theta$$
$$+ 4\, \mathrm{Re}\, \rho^{K^*}_{1,0}(\theta) \cos^2\Theta$$

Since $\rho^{K^*}(\Theta, \theta)$ satisfies the same symmetry relations as $\rho^{K^*}(\theta)$, the four matrix elements given in Eq. (A. 2), completely specify $\rho^{K^*}(\Theta, \theta)$.

Appendix B

Experimentally ρ^{K*} can only be determined integrated over some finite interval of production angles. Let the integration interval be $\alpha \leq \cos\theta \leq \beta$. The ensuing real integrals are defined:

$$S_{2\lambda,2\lambda'} = \int_\alpha^\beta d\cos\theta \; Q_{2\lambda,2\lambda'}$$

$$S^{(1)}_{2\lambda,2\lambda'} = \int_\alpha^\beta d\cos\theta \; Q_{2\lambda,2\lambda'} \sin 2\Theta \qquad \text{(B.1)}$$

$$S^{(2)}_{2\lambda,2\lambda'} = \int_\alpha^\beta d\cos\theta \; Q_{2\lambda,2\lambda'} \cos^2\Theta$$

In Eq. (B.1) the pair of indices 2λ, $2\lambda'$ runs through the values 1,1; 3,3; 3,1; and 3,-1. The functions $Q_{2\lambda,\,2\lambda'}$ of θ have been defined in Eqs. (4) and (10). Inserting Eq. (12) into Eq. (A. 2) and making use of the definition (B. 1) the integrated matrix ρ^{K*} is obtained in a form which gives it dependence on the helicity amplitudes:

$$\begin{aligned}
2\rho^{K*}_{1,\pm1} &= |T_{1,\frac12}|^2\{S_{1,1} \pm S^{(2)}_{1,1}\} + |T_{1,-\frac12}|^2\{S_{3,3} \pm S^{(2)}_{3,3}\} + \\
&\pm 2|T_{0,\frac12}|^2\{S_{1,1} - S^{(2)}_{1,1}\} + 2\eta\,\mathrm{Re}\{T_{1,\frac12}T^*_{1,-\frac12}\} \times \\
&\{S_{3,-1} \mp S^{(2)}_{3,-1}\} \pm \sqrt2\,\eta\,\mathrm{Re}\{T_{1,-\frac12}T^*_{0,\frac12}\}S^{(1)}_{3,1} \\
\rho^{K*}_{0,0} &= |T_{1,\frac12}|^2\{S_{1,1} - S^{(2)}_{1,1}\} + |T_{1,-\frac12}|^2\{S_{3,3} - S^{(2)}_{3,3}\} + \qquad \text{(B.2)} \\
&+2|T_{0,\frac12}|^2 S^{(2)}_{1,1} - 2\eta\,\mathrm{Re}\{T_{1,\frac12}T^*_{1,-\frac12}\}\{S_{3,-1} - S^{(2)}_{3,-1}\} + \\
&-\sqrt2\,\eta\,\mathrm{Re}\{T_{1,-\frac12}T^*_{0,\frac12}\}S^{(1)}_{3,1} \\
2\rho^{K*}_{1,0} &= -\tfrac12\sqrt2\,|T_{1,\frac12}|^2 S^{(1)}_{1,1} - \tfrac12\sqrt2\,|T_{1,-\frac12}|^2 S^{(1)}_{3,3} + \sqrt2\,|T_{0,\frac12}|^2 S^{(1)}_{1,1} \\
&+\sqrt2\,\eta\,\mathrm{Re}\{T_{1,\frac12}T^*_{1,-\frac12}\}S^{(1)}_{3,-1} + 4\eta\,\mathrm{Re}\{T_{1,-\frac12}T^*_{0,\frac12}\}S^{(2)}_{3,1} \\
&-2\eta\,T^*_{1,-\frac12}T_{0,\frac12}\,S_{3,1}
\end{aligned}$$

Again Eq. (B. 2) completely specifies ρ^{K*}. The contributing products of helicity amplitudes are weighted by suitable combinations of integrals S. These integrals are discussed in Appendix D.

Appendix C

As should be expected $\mathrm{Tr}\rho^{K*} = \int_{\alpha}^{\beta} d\cos\theta \,\mathrm{Tr}\,\rho^{K*}(\theta) = \int_{\alpha}^{\beta} d\cos\theta\, W$ In order to obtain the matrix ρ with $\mathrm{Tr}\,\rho = 1$, studied experimentally, ρ^{K*} has to be divided by:

$$D = 2\left\{|T_{1,\frac{1}{2}}|^2 + |T_{0,\frac{1}{2}}|^2\right\} S_{1,1} + 2|T_{1,-\frac{1}{2}}|^2 S_{3,3} \qquad \text{(C. 1)}$$

So finally one has:

$$\rho = \frac{\rho^{K*}}{D} \qquad \text{(C. 2)}$$

where ρ^{K*} and D as functions of the helicity amplitudes are given by Eqs. (B. 2) respectively (C. 1).

Appendix D

In view of the high momenta of K^- as well as of K^* in the overall cm system, the connection between Θ and θ has to be determined relativistically. As is well known this is most conveniently achieved by application of hyperbolic trigonometry in a triangle the basis of which has length argtgh v_{K^-} ; a side of which has length argtgh v_{K*} and of which the angle subtended by these two sides equals θ. The external angle at the top then is Θ. The "cosine" and "sin" rules thus yield:

$$\sin\Theta = \sin\theta \sqrt{\frac{1 - v_{K^*}^2}{1 - 2\beta\cos\theta + \beta^2 - v_{K^*}^2 \sin^2\theta}} \qquad \text{(D. 1)}$$

where v_{K^*} is the K^* velocity in units of c, and $\beta = \frac{v_{K^*}}{v_{K^-}}$, v_{K^-} being similarly the K^- velocity, both velocities measured in the overall cm system. For the incident momentum 1.5 GeV/c one has $\beta \approx 0.5$ and $v_{K^*} \approx 0.41$. On the intervals $-1 \leq \cos\theta \leq -\frac{1}{3}$ as well as on $-\frac{1}{3} \leq \cos\theta \leq \frac{1}{3}$, but not on $\frac{1}{3} \leq \cos\theta \leq 1$, the two quadratic terms in the denominator in the right-hand side of Eq. (D.1) may be neglected within 5 per cent accuracy in $\sin\Theta$. As a consequence one has within a few per cent accuracy:

$$4 \sin\Theta = 5 \cos\tfrac{1}{2}\theta \qquad \text{for } \cos\theta < \tfrac{1}{3} \tag{D.2}$$

The advantage of Eq. (D.2) with respect to Eq. (D.1) is that it allows for a calculation of the integrals S, Eq. (B.1), in an elementary way. The precision is sufficient for the purpose of the analysis described in the text.

Finally the functions $Q_{2\lambda,2\lambda'}$, which figure in the definition of the integrals S, may be given explicitly for $J = \frac{5}{2}$ and $M = \frac{1}{2}$. Eqs. (4) and (5) yield:

$$\begin{aligned} Q_{1,1} &= \tfrac{1}{2} + \tfrac{4}{7} P_2 + \tfrac{3}{7} P_4 \\ Q_{3,3} &= \tfrac{1}{2} + \tfrac{1}{7} P_2 - \tfrac{9}{14} P_4 \\ Q_{3,1} &= -\tfrac{1}{28}\sqrt{2}\left\{4 P_2' + 3 P_4'\right\} \\ Q_{3,-1} &= -\tfrac{1}{56}\sqrt{2}\left\{6 P_2^2 + P_4^2\right\} \end{aligned} \tag{D.3}$$

One notices that $Q_{1,1}$, $Q_{3,3}$ and $Q_{3,-1}$ are (rational) symmetric functions of $\cos\theta$, whereas $Q_{3,1}$ is (irrational and) odd in $\cos\theta$. On symmetric intervals $\alpha = -\beta$, one has $S_{3,1} = 0$ therefore, but all other integrals S are non-zero in general. Eq. (B.2) then shows that on symmetric intervals $\rho_{1,0}$ has to be real, in which case the K^* spin density matrix is real. In that case the K^* disintegration angular distribution alone, or equivalently $\rho_{0,0}$, λ and γ, completely determine ρ, in the one isobar hypothesis.

ACKNOWLEDGEMENTS

The author is indebted to the International Atomic Energy Agency, and in particular to the director of the International Centre for Theoretical Physics, Professor Abdus Salam, for a profitable stay at I C T P, Trieste. This work partially belongs to the research programme of the "Stichting voor Fundamenteel Onderzoek der Materie" F. O. M., financially supported by the "Nederlandse Organisatie voor Zuiver Wetenschappelijk Onderzoek", Z. W. O. He wishes to thank Professors J. Kluyver and S. Wouthuysen for their continuous interest in this work. He gratefully acknowledges some discussions on the subject with Professors A. O. Barut, S. Berman, K. Nishijima and J. Werle at I C T P.

REFERENCES

1) A recent account of the peripheral model applied to inelastic resonance production is : The Peripheral Model with Form Factors, G. C. FOX. Preprint Department of Applied Mathematics and Theoretical Physics, University of Cambridge, Cambridge, England, February 1965.

One pion exchange in the processes $KN \to NK^*$ has been calculated in detail e.g. by V. BERZI, E. RECAMI, Preprint Instituto di Fisica dell'Università, Milano, IFUM - 010/Sp, March 1965.

2) K. GOTTFRIED, J. JACKSON, Nuovo Cimento 33,(1964) 309.

J. JACKSON, H. PILKUHN, Nuovo Cimento 33, (1964) 906, with erratum in Vol. 34 (1964) 1841.
J. JACKSON, Nuovo Cimento 34 (1964) 1644.

M. FERRO-LUZZI, R. GEORGE, Y. GOLDSCHMIDT-CLERMONT, V. HENRI, B. JONGEJANS, D. LEITH, G. LYNCH, F. MULLER, J. PERREAU, Preprint CERN/TC/Physics 65-6, February 1965. To be published in Nuovo Cimento.

3) Ph. SALIN, Nuovo Cimento 28 (1963) 1384.

C. HÖHLER, W. SCHMIDT, Annals of Physics, 28 (1964) 34.

4) G. SMITH, J. SCHWARTZ, D. MILLER, G. KALBFLEISCH, R. HUFF, O. DAHL, G. ALEXANDER, Phys. Rev. Letters 10 (1963) 138.

G. CHADWICK, D. CRENNELL, W. DAVIES, H. DERRICK, J. MULVEY, P. JONES, D. RADOJICIC, C. WILKINSON, A. BETTINI, H. CRESTI, S. LAMENTANI, L. PERRUZZO, R. SANTANGELO, Physics Letters 6 (1963) 309.

H. FERRO-LUZZI, R. GEORGE, Y. GOLDSCHMIDT-CLERMONT, V. HENRI, B. JONGEJANS, D. LEITH, G. LYNCH, F. MULLER, J. PERREAU, Proc. of the Sienna International Conf. on Elementary Particles, Vol. I (1963)188.

5) K. GOTTFRIED, J. JACKSON, Nuovo Cimento 34 (1964) 735, with erratum in Vol. 34 (1964) 1843.

M. FERRO-LUZZI et al., viz. Ref. 2.

6) K. DIETZ, H. PILKUHN, Preprint CERN 10013/TH. 450, December 1964.

7) W. COOPER, H. FILTHUTH, A. FRIDMAN, E. MALAMUD, H. SCHNEIDER, E. GELSEMA, J. KLUYVER, A. TENNER, Proc. of the Sienna Int. Conf. on Elementary Particles, Vol. I (1963) 160.

8) R. ADAIR, Preprint CERN/TH/63-12, July 1963, Background Amplitudes and the spin of the Y_1^* .

9) A similar suggestion has been made by E. MALAMUD, P. SCHLEIN, Physics Letters 10 (1964) 145.

10) Diagrams assumed to contribute to the reaction $\pi^+ p \rightarrow \Sigma^+ K^+$ are the ones for one K^* exchange; intermediate isobars $N_{\frac{3}{2}}^*$ (1238) and $N_{\frac{3}{2}}^*$ (1920); respectively an uncrossed isobar diagram with a Λ hyperon in the intermediate state. This model yields satisfactory fits to differential cross-section and Σ^+ polarization from threshold to 1.8 GeV/$_c$ incident momentum (Lab). L. EVANS, J. KNIGHT, Phys. Rev. 137 (1965) B1232. A simpler case is the reaction $\pi^+ N \rightarrow \Sigma K^{*+}$ as studied by C. H. CHAN, Y. LIU, Nuovo Cim. 35 (1965) 298.

11) Compare e. g. M. ROOS, Nuclear Physics, 52 (1964) 1, or A. G. TENNER, G. F. WOLTERS, Progress of Elementary Particle and Cosmic Ray Physics, to be published.

12) J. BADIER, H. DEMOULIN, J. GOLDBERG, B. GREGORY, P. KREJBICH, C. PELLETIER, H. VILLE, R. BARLOUTAUD, A. LEVEQUE, C. LOUEDEC, J. MEYER, P. SCHLEIN, E. GELSEMA, W. HOOGLAND, J. KLUYVER, A. TENNER, Proc. of the 1964 Dubna Int. Conf. on High Energy Physics, to be published.

13) G. CHADWICK et al., viz. Ref. 4.

14) M. FERRO-LUZZI et al., viz Refs. 2 and 4.

15) E. GELSEMA, J. KLUYVER, A. TENNER, G. WOLTERS Physics Letters 10 (1964) 341.

16) A detailed description of the experiment in question is given by E. GELSEMA, doctoral thesis, University of Amsterdam, Amsterdam, to be published.

17) M. JACOB, G. C. WICK, Annals of Physics 7 (1959) 404. Description of disintegrations in helicity representation has earlier been given by M. JACOB, Nuovo Cimento 9 (1958) 826.

18) Numerical values have been taken from: M. ROTENBERG, R. BIVINS, N. METROPOLIS, J. WOOTEN Jr., the 3-j and 6-j symbols, the Technology Press, MIT, Cambridge, Massachusetts, 1959.

19) G. WOLTERS, Proc. Kon. Ned. Acad. Wetenschappen, Series B, 67 (1964) 192.

Note added in proof:

It was mentioned in connection with the ambiguities in the helicity amplitudes that parity of the intermediate isobar does not follow from $\rho_{0,0}$, λ and γ alone. The transverse proton polarization in the final state does not resolve this ambiguity. This may be seen as follows:

From Eq. 2 one finds $< s_y >= -W^{-1}\, 2\mathrm{Im}\{T_{1,\frac{1}{2}}\, T^{*}_{1,-\frac{1}{2}}\}\, Q_{1,3}$
Hence the substitutions $T_{1,-\frac{1}{2}} \rightarrow T^{*}_{1,-\frac{1}{2}}$; $T_{1,\frac{1}{2}} \rightarrow - T^{*}_{1,\frac{1}{2}}$; $T_{0,\frac{1}{2}} \rightarrow - T^{*}_{0,\frac{1}{2}}$ and $\eta \rightarrow -\eta$ leave invariant $W, \rho_{0,0}, \lambda, \nu$ as well as $< s_y >$. Measurement of the transverse proton polarization yields in principle a sharp test of the "one isobar" hypothesis, since the dependence of $< s_y >$ on θ is predicted completely, and will still be interesting therefore. It is noticed however, that the best fits to the data analysed before, imply $\mathrm{Im}\{T_{1,\frac{1}{2}}\ T^{*}_{1,-\frac{1}{2}}\}$ to be almost zero or to vanish here.

FIGURE CAPTIONS

Fig. 1. a. Uncrossed isobar diagram for $Y_1^{*\pm}$ production in K^-p collisions.

Fig. 1. b. Crossed isobar diagram for $Y_1^{*\pm}$ production in K^-p collisions.

Fig. 2. Histogram for K^* production angular distribution in the reaction $K^-p \rightarrow pK^{*-}$, at 1.5 GeV/$_c$ incident momentum (Lab.). Predicted curves showing the agreement in the backward hemisphere for $0 \leq T \leq 0.37$. The curves 1 through 4 correspond to $T = 0.37$; 0.28; 0.14 and 0 respectively.

Fig. 3. The optimal fits to K^* spin density matrix parameters for $0 \leq T \leq 0.37$. The values of r(T), s(T) and t(T) are measured on the left-hand side ordinate axis; those of the corresponding minimal $X^2(T)$ on the right-hand side ordinate axis.

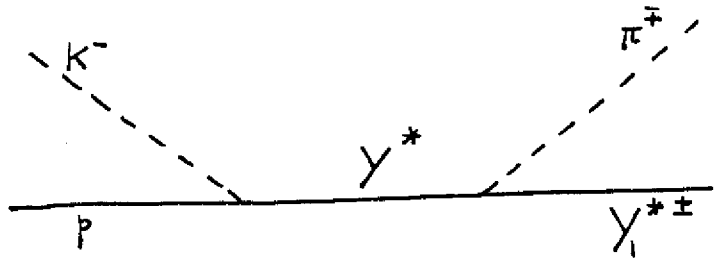

Fig. 1 a

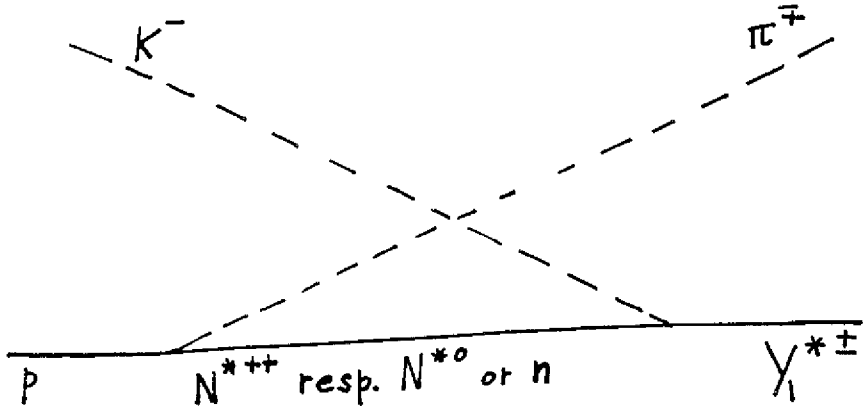

Fig. 1 b

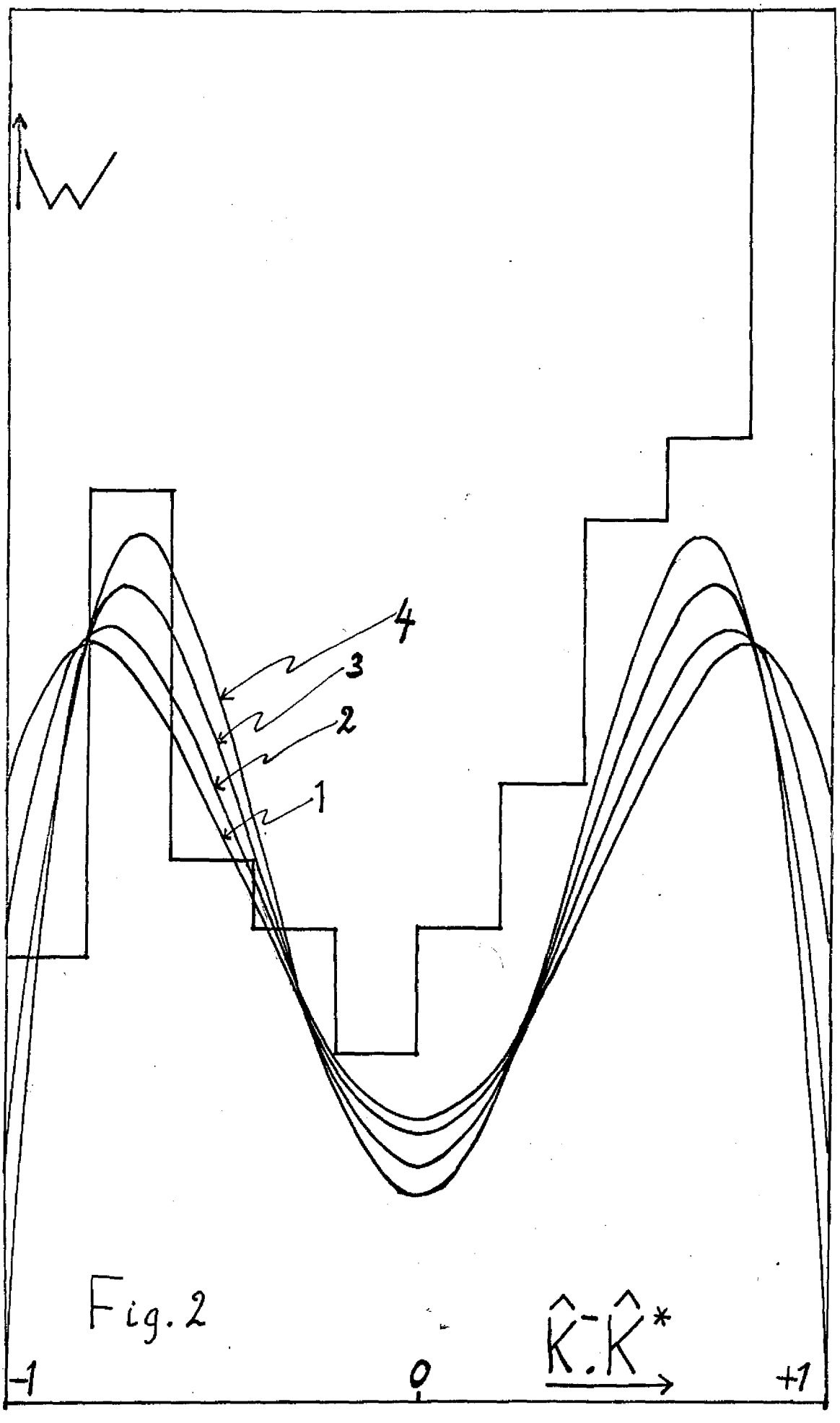

Fig. 2

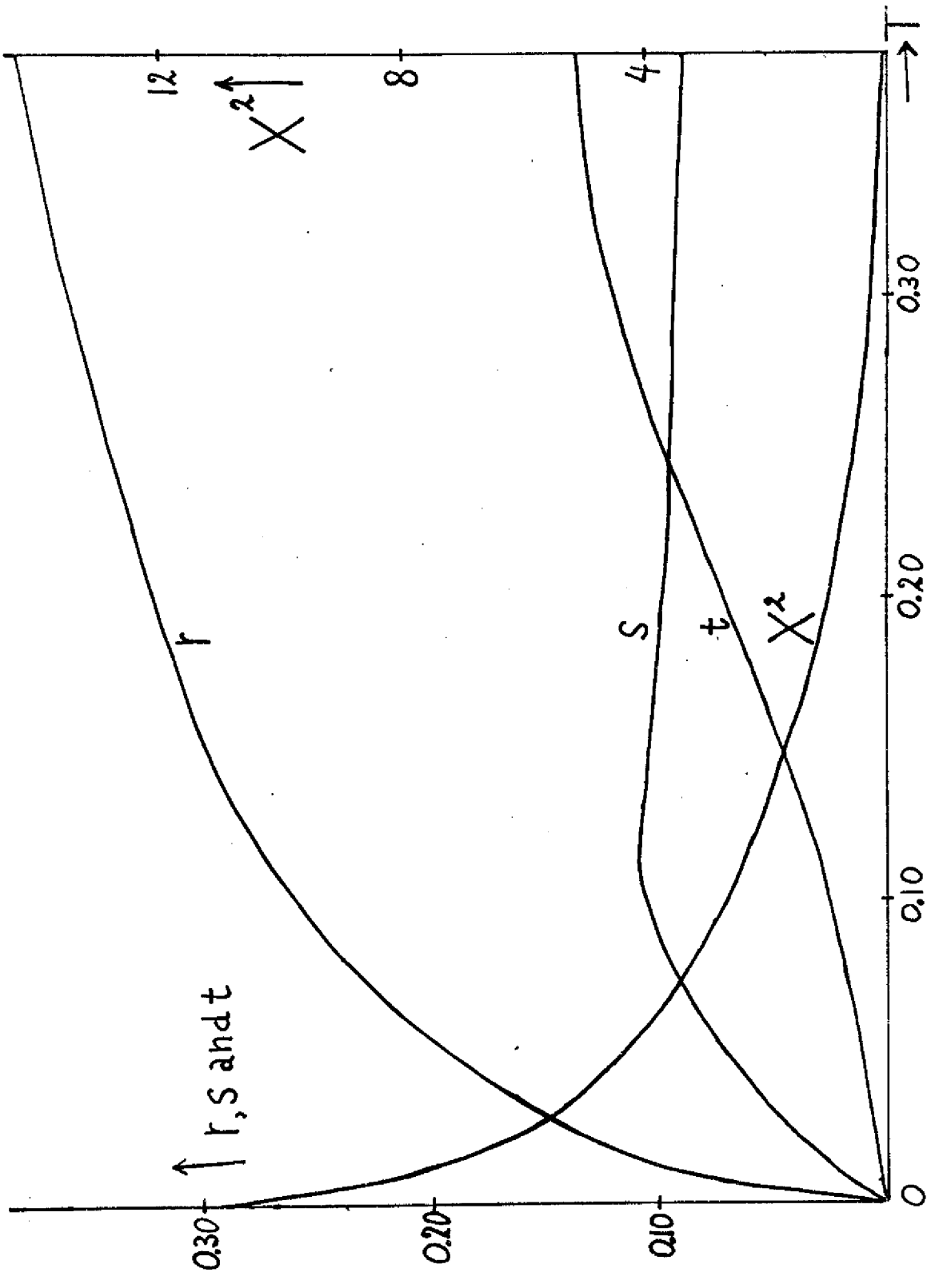

Fig. 3